The Evaporative Demand Drought Index. Part I: Linking Drought Evolution to Variations in Evaporative Demand

MICHAEL T. HOBBINS,[a,b] ANDREW WOOD,[c] DANIEL J. MCEVOY,[d] JUSTIN L. HUNTINGTON,[d]
CHARLES MORTON,[d] MARTHA ANDERSON,[e] AND CHRISTOPHER HAIN[f]

[a] Cooperative Institute for Research in Environmental Sciences, University of Colorado Boulder, Boulder, Colorado
[b] NOAA/Earth Systems Research Laboratory/Physical Sciences Division, Boulder, Colorado
[c] National Center for Atmospheric Research, Boulder, Colorado
[d] Desert Research Institute, Reno, Nevada
[e] Hydrology and Remote Sensing Laboratory, Agricultural Research Service, U.S. Department of
Agriculture, Beltsville, Maryland
[f] Earth System Science Interdisciplinary Center, University of Maryland, College Park, College Park, Maryland

ABSTRACT

Many operational drought indices focus primarily on precipitation and temperature when depicting hydroclimatic anomalies, and this perspective can be augmented by analyses and products that reflect the evaporative dynamics of drought. The linkage between atmospheric evaporative demand E_0 and actual evapotranspiration (ET) is leveraged in a new drought index based solely on E_0—the Evaporative Demand Drought Index (EDDI). EDDI measures the signal of drought through the response of E_0 to surface drying anomalies that result from two distinct land surface–atmosphere interactions: 1) a complementary relationship between E_0 and ET that develops under moisture limitations at the land surface, leading to ET declining and increasing E_0, as in sustained droughts, and 2) parallel ET and E_0 increases arising from increased energy availability that lead to surface moisture limitations, as in flash droughts. To calculate EDDI from E_0, a long-term, daily reanalysis of reference ET estimated from the American Society of Civil Engineers (ASCE) standardized reference ET equation using radiation and meteorological variables from the North American Land Data Assimilation System phase 2 (NLDAS-2) is used. EDDI is obtained by deriving empirical probabilities of aggregated E_0 depths relative to their climatologic means across a user-specific time period and normalizing these probabilities. Positive EDDI values then indicate drier-than-normal conditions and the potential for drought. EDDI is a physically based, multiscalar drought index that that can serve as an indicator of both flash and sustained droughts, in some hydroclimates offering early warning relative to current operational drought indices. The performance of EDDI is assessed against other commonly used drought metrics across CONUS in Part II.

1. Introduction

a. Drought, ET, and E_0

Drought severely affects society, ecology, and economies, with impacts felt across sectors and hydrologic and political boundaries at time scales that vary from weeks to years. Across sectors, drought is essentially an extended imbalance between moisture supply and demand—relative to long-term mean conditions for the period in question—in favor of demand. Physically, it is manifest as deficits in moisture fluxes and storages, including precipitation (Prcp) in meteorological drought; streamflow [runoff (RO)] and surface storage depletion in hydrologic drought; and, traditionally, evapotranspiration (ET) and soil moisture (SM) in agricultural drought. Agricultural and meteorological droughts are also revealed as a surplus in atmospheric evaporative demand E_0 (also sometimes referred to as "potential evaporation"). The E_0 physically integrates radiative and advective forcing variabilities and, further, reflects water availability through land surface–atmosphere feedbacks that affect partitioning of the available energy at the surface into latent and sensible heat fluxes. Across the energy-limited range of the hydroclimatic spectrum, E_0

Corresponding author address: Michael Hobbins, NOAA/ESRL/
Physical Sciences Division, 325 Broadway, Boulder, CO 80305.
E-mail: mike.hobbins@noaa.gov

drives ET, while in the water-limited range, E_0 is driven by ET. In this way, the two measures—one ideal (E_0) and the other actual (ET)—together reflect the full range of evaporative drivers and responses to drought. ET and E_0 together offer reciprocal perspectives on drought, with E_0 acting as a strong indicator of potential drought conditions (conditions that may or may not eventuate, depending on mitigating factors such as irrigation management), whereas drought evaporative impacts may be better measured by an independent measure of ET. However, in many regions and operational settings, ET is derived from E_0 through parameterizations of soil-water and plant-water availabilities that are of questionable value on operational space and time scales: in such cases E_0 may serve as an independent drought indicator.

b. Existing drought-monitoring tools

Most drought monitoring concentrates on the supply side of the moisture imbalance. Indeed, the current iteration of the U.S. Drought Monitor (USDM)—the most widely used operational drought-monitoring tool in the United States—relies heavily on drought indicators that are themselves driven by Prcp alone [such as the Standardized Precipitation Index (SPI); McKee et al. 1993] or by Prcp and air temperature T_{air} data [such as in the Palmer drought severity index (PDSI); Palmer 1965] to derive drought category assessments and other ancillary products such as surface moisture fluxes. In the latter type of assessment, E_0 is generally used in an implicit manner to derive ET fluxes through land surface models (LSMs) but is not an explicit input to the USDM. Instead, simple formulations based on T_{air} alone are used: the PDSI employs a Thornthwaite-like T_{air}-based E_0 (Thornthwaite 1948); the "leaky bucket" Climate Prediction Center (CPC) soil moisture model (Huang et al. 1996) uses the T_{air}-based Hargreaves reference ET (Hargreaves and Samani 1985). However, the choice of E_0 formulation for bucket models significantly affects both the magnitude and direction of short- and long-term trends in estimated ET and SM, particularly in energy-limited areas (Hobbins et al. 2008). For instance, T_{air}-based E_0 measures show declines in long-term ET (i.e., drying) as T_{air} rises (Dai et al. 2004), in opposition to worldwide [and contiguous United States (CONUS)] observed trends (Hobbins et al. 2004; Roderick et al. 2009). Furthermore, a number of studies show that T_{air} is often not the most significant driver of long-term E_0 trends (e.g., Roderick et al. 2007). For example, while the short-term (daily) variability of E_0 during the critical growing season is dominated by T_{air} over most of CONUS, it is notably most strongly influenced by wind speed U in the southwest and downwelling shortwave radiation R_d in the southeast (Hobbins et al. 2012; Hobbins 2016). Arguably, more physically explicit E_0 formulations—such as those based on the Penman (1948) combination equation—will more accurately reflect observations of both wetting and drying under warming (Hobbins et al. 2008; Sheffield et al. 2012).

c. Emerging evaporation-based drought-monitoring tools

Within the drought-monitoring community, attention is turning toward the demand side of the moisture imbalance, as several drought indices predicated on the drought signal of physically based ET are emerging [e.g., the Soil Moisture Deficit Index and Evapotranspiration Deficit Index (Narasimhan and Srinivasan 2005); the standardized precipitation evapotranspiration index (SPEI; Vicente-Serrano et al. 2010); the evaporative stress index (ESI; Anderson et al. 2007); the remotely sensed global drought severity index (Mu et al. 2013); and the optimal blended North American Land Data Assimilation System (NLDAS) drought index (Xia et al. 2014)]. However, while E_0 could be a flexible driver in drought monitoring—it may be remotely sensed, land based, or physically observed, and it does not rely on LSMs—no indices relating to E_0 alone yet exist. While SPEI monitors drought based on the difference between supply (Prcp) and demand (E_0 from reference ET), the particular reference ET measure used is based on T_{air}. An index based solely on a physically based E_0 measure would have several advantages: characterization of the surface water availability is obviated, as are difficulties intrinsic to remotely sensed data streams such as data availability delays and the requisite infilling of data because of satellite-overpass intervals or cloud cover.

Such an index could help fill a gap between science and applications in that it would be operationally tractable for detecting and monitoring both flash and sustained droughts with negligible latency (we define "latency" as the period between the occurrence of a phenomenon and when usable data about it become available). However, reference ET derived from reanalysis data is subject to inherited uncertainties because of spatial interpolation and data assimilation techniques that underpin the reanalysis, and the concept relies on surface assumptions that may be contravened under nonirrigated or dry environments.

d. ET−E_0 relations in drought

Depending on whether ET is limited by the availability of energy or of water, E_0 either plays a role in determining ET or else is reflective of ET. In non-water-limited conditions, E_0 estimates the upper limit of (energy limited) ET, whereas in water-limited conditions,

land–atmosphere feedbacks generated from ET drive E_0 in an opposite, or complementary, direction. Clearly, in sustained drought (i.e., sustained deficits in SM and associated fluxes at the land–atmosphere interface), the water limit applies to ET. This is less often true, however, in the case of "flash drought" (i.e., fast-developing drought driven by strong, transient meteorological/radiative changes—such as increases in T_{air}, wind, or radiation, or decreases in humidity—with no substantive change in Prcp). Nonetheless, the positive E_0 signal manifested in both sustained and flash droughts suggests that E_0 has value both for monitoring droughts and as a leading indicator of developing drought conditions.

In this paper, we offer a physical rationale for an E_0-based drought index and propose an index formulation, termed the Evaporative Demand Drought Index (EDDI). The performance of EDDI is assessed across CONUS in a companion paper (McEvoy et al. 2016a, hereafter Part II). Here, we develop the theoretical basis of EDDI and demonstrate how the E_0 connection to drought makes it not only a useful drought metric but also provides for attribution of drought evolution into its individual meteorological forcings. We compare EDDI to the USDM in case studies of flash and sustained droughts in basins drawn from across CONUS's hydroclimatic spectrum. We also examine EDDI's long-term performance as a leading drought indicator and close with discussion and conclusions that motivate the more complete assessment in Part II.

2. Physical rationale for an E_0-based drought indicator

a. Derivation of E_0

For E_0 we use the American Society of Civil Engineers (ASCE) standardized reference ET equation (Allen et al. 2005), which provides a widely accepted estimate of E_0 derived from the Penman–Monteith equation (Monteith 1965). It takes the form of a weighted combination of two driving terms: a radiative term [the first term on the right-hand side of Eq. (1)], reflecting the energy availability at the evaporating surface, and an advective term (second term), reflecting the ability of the overpassing air to absorb and carry away evaporated moisture. The equation is as follows:

$$E_0 = \frac{0.408\Delta}{\Delta + \gamma(1 + C_d U)}(R_n + L_n - G)\frac{86\,400}{10^6}$$

$$+ \frac{\gamma\dfrac{C_n}{T_{air}}}{\Delta + \gamma(1 + C_d U)}U\frac{e_{sat} - e_a}{10^3}, \tag{1}$$

where E_0 (mm day^{-1}) is atmospheric evaporative demand; Δ (Pa K^{-1}) is the slope of the saturated vapor pressure–temperature curve at the 2-m air temperature (K); γ (Pa K^{-1}) is the psychrometric constant; U (m s^{-1}) is the wind speed (here specified at a 2-m height); R_n (W m^{-2}) and L_n (W m^{-2}) are the net incoming shortwave and longwave radiation, respectively; G (W m^{-2}) is the downward ground heat flux; e_{sat} (Pa) and e_a (Pa) are the saturated and actual vapor pressures, respectively; C_n (K mm s^3 Mg^{-1} day^{-1}) and C_d (s m^{-1}) are the "numerator constant" and "denominator constant," respectively, with values defined in Allen et al. (2005); and the 0.408 term (m^2 mm MJ^{-1}) represents the inverse of the latent heat of vaporization (normally λ), converting E_0 to daily depth units. The remaining terms convert from SI units to those specified in Allen et al. (2005): the 86 400/10^6 term converts the first term on the right-hand side (from W m^{-2} to MJ m^{-2} day^{-1}), and the 10^3 denominator converts the vapor pressure deficit (VPD; defined as $e_{sat} - e_a$) in the numerator (from Pa to kPa).

Reference conditions are assumed to be a well-watered, 0.5-m alfalfa crop, actively growing and completely shading the ground with a constant albedo of 0.23 (though one could also use the 0.12-m grass reference crop, requiring different values for C_n and C_d). Although not explicit in Eq. (1), the ASCE version of the Penman–Monteith equation for reference ET implicitly assumes a surface resistance of 45 s m^{-1} (70 s m^{-1} for the 0.12-m grass reference crop).

b. Complementary and parallel interactions of ET and E_0

The complementary and parallel interactions of ET and E_0 in both sustained and flash droughts form the physical basis for EDDI, with the physical linkage between drought and E_0 resulting from one of two dynamics, depending on the prevailing hydroclimate. In the first, under moist, energy-limited ET conditions, variations in surface energy Q_n [the sum of the fluxes of sensible heat H and latent heat (λET) to the atmosphere (in this section, we specify λET and λE_0 as the energy equivalents of the mass fluxes ET and E_0, respectively)] cause both ET and E_0 to vary proportionally to Q_n. Second, under water-limited ET conditions, variability in ET drives a complementary variability in E_0 through energetic interactions across the land–atmosphere interface. This latter dynamic is known as the "complementary relationship" (Bouchet 1963): when ET becomes water limited, Q_n is repartitioned to favor H over λET. The increased H raises the VPD of the dynamic boundary layer and thereby increases E_0. The general form of the complementary relationship is
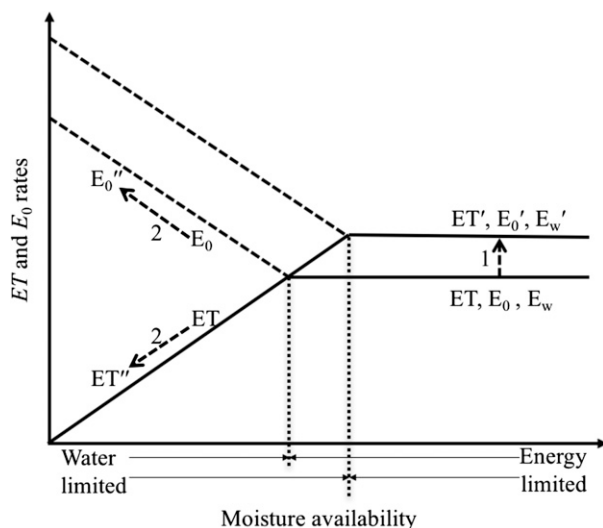
$$ET = kE_w - E_0, \tag{2}$$

FIG. 1. Idealized parallel and complementary responses of ET and E_0 to varying moisture and energy conditions shown within the Budyko (1974) framework. Arrows represent variations from normal conditions for ET and E_0: the arrow marked 1 shows parallel responses, with ET and E_0 increasing to ET′ and E_0' respectively, under drying in energy-limited conditions, such as under flash drought; the arrows marked 2 show complementary responses, with ET decreasing to ET″ while E_0 increases to E_0'' under drying in already water-limited conditions, such as in extended drought.

where E_w is the ET rate for a regional-scale wet surface, most often derived from the Priestley–Taylor expression (Priestley and Taylor 1972), with k a positive number most often assumed to be 2, which assumes that the energy released at the surface by declining λET raises E_0 by as much as λET falls.

These two dynamics—that is, parallel and complementary ET−E_0 relations—are illustrated in Fig. 1, which shows ET and E_0 converging on E_w with increasing moisture availability. The dynamics have been observed acting across CONUS: Hobbins et al. (2004) showed that trends in the driving dynamics of E_0 and ET lead to trends in ET that corroborate both complementary and parallel ET−E_0 relations.

EDDI uses observations of both dynamics to indicate droughts of various types. In flash drought, moisture changes lag behind changes in meteorological drivers (e.g., increasing T_{air}), causing a transient period during which SM decreases slowly, leaving moisture still available for ET, while the energy to drive ET increases; this leads to rises in both λET and λE_0, as indicated by the dashed arrow "1" in Fig. 1. Mo and Lettenmaier (2015) refer to this type of drought as a "heat wave flash drought" (as distinct from flash droughts driven by rapid Prcp declines) and define it as driven by high T_{air}; we maintain that these droughts may also be driven by the

other drivers of E_0 and ET, for example, low specific humidity q or high R_d or U. Whatever the meteorological or radiative forcing, in the early stages of flash drought, E_0 and ET will increase together, with elevated E_0 anomalies leading EDDI to indicate the potential onset of drought. As drying progresses, the elevated ET depletes SM. Eventually, in a sustained drought, ET declines in response to an increasingly limited moisture supply (lower dashed arrow "2" in Fig. 1). In this phase, holding all else equal, Q_n favors increasing H, which heats the dynamic boundary layer and raises its VPD, thereby increasing λE_0 (upper dashed arrow "2" in Fig. 1). Further, under sustained drought, regional cloudiness decreases and R_d (or Q_n) increases. (These large- and small-scale dynamics between regional ET and E_0 underpin the classical understanding of the complementary relationship.)

That E_0 increases in both flash droughts and sustained drought, whereas ET responds to these two drought types in opposite directions, demonstrates the robustness of E_0 as an indicator of droughts of different origins. Central to EDDI is the concept that during both flash droughts and sustained droughts E_0 should demonstrate a surplus relative to its climatological mean. As a drought progresses, this surplus should accumulate, dissipating only when, for a sustained period, moisture availability exceeds its climatological levels or the meteorologic and/or radiative drivers at the surface result in E_0 falling below its climatological mean.

3. Methods and data

a. EDDI formulation

The single probability distributions used in parametric methods (such as the Gamma distribution for the SPI) may not always be appropriate for climatic time series at large spatial scales (Guttman 1999; Quiring 2009; Vicente-Serrano et al. 2012), so EDDI uses a nonparametric approach, in which empirically derived probabilities are obtained through an inverse normal approximation (Abramowitz and Stegun 1965). This probability-based approach allows for more consistent comparisons between EDDI against other standardized indices (Farahmand and AghaKouchak 2015).

First, E_0 probabilities $P(E_{0_i})$ across a period of interest are obtained through the empirical Tukey plotting position (Wilks 2011):

$$P(E_{0_i}) = \frac{i - 0.33}{n + 0.33}, \qquad (3)$$

where $P(E_{0_i})$ is the empirical probability of E_{0_i}, which is aggregated across the period of interest (e.g., to

TABLE 1. Characteristics and hydroclimates of the four example basins used in this study.

USGS gauge name (number)	Contributing area (km^2)	Gauge elevation (m)	Mean annual hydroclimate (2000–13)				
			Prcp (mm)	ET (mm)	E_0 (mm)	Aridity index E_0/Prcp	Evaporation index ET/Prcp
Allegheny River at Natrona, PA (03049500)	29 550	225	1094	678	1098	1.00	0.62
Current River at Doniphan, MO (07068000)	5278	98	1258	779	1623	1.29	0.62
Russian River near Ukiah, CA (1146100)	260	183	1005	810	2112	2.10	0.81
Colorado River near Cisco, UT (09180500)	61 770	1247	494	729	1509	3.05	1.47

estimate a 2-month EDDI on 31 January, E_0 is summed over the period from 1 December to 31 January); i is the rank of the aggregated E_0 in the historical time series ($i = 1$ for maximum E_0); and n is the number of observations in the series being ranked. (For analysis of a period within the climatology, n is the climatology length in years; for periods outside the climatology, n is augmented by 1. In an operational setting, n increases as the climatology is updated with time.) EDDI is then derived following the inverse normal approximation detailed in Vicente-Serrano et al. (2010), repeated here for convenience:

$$\text{EDDI} = W - \frac{C_0 + C_1 W + C_2 W^2}{1 + d_1 W + d_2 W^2 + d_3 W^3}. \qquad (4)$$

The constants are defined as follows: $C_0 = 2.515\,517$, $C_1 = 0.802\,853$, $C_2 = 0.010\,328$, $d_1 = 1.432\,788$, $d_2 = 0.189\,269$, and $d_3 = 0.001\,308$. For $P(E_{0_i}) \leq 0.5$, $W = \sqrt{-2\ln[P(E_{0_i})]}$, and for $P(E_{0_i}) > 0.5$, replace $P(E_{0_i})$ with $[1 - P(E_{0_i})]$ and reverse the sign of EDDI.

A zero EDDI value indicates that E_0 accumulated over the aggregation period in the year of interest is equal to the median value from the climatology; negative values indicate wet anomalies, and positive values indicate drier-than-normal conditions, with drought intensity increasing with increasingly positive EDDI. The range of EDDI is a function of n: in the case of estimating EDDI within our climatology period (1980–2015), $n = 36$, so EDDI has a range of ± 2.09.

EDDI is multiscalar in space and time: it may be estimated at a point (or pixel) or by using spatial-mean E_0 over a region, and aggregation periods may vary from as little as one day to a year or more, similar to other multiscalar drought indices such as the SPI. Appropriate period lengths would be tailored to the regional hydroclimatology, sector, user interest, and other criteria (see section 4c).

b. Input data

For the CONUS-wide reanalysis of E_0 from Eq. (1), daily inputs are temporally aggregated from the following hourly fields from NLDAS phase 2 (NLDAS-2;

Xia et al. 2012): 2-m T_{air} (K), 2-m q (kg kg^{-1}), station pressure P_a (Pa), R_d (W m^{-2}), and the two orthogonal horizontal 10-m wind vector components U_x and U_y (m s^{-1}; U_x and U_y are converted to a scalar hourly wind speed before temporal aggregation). The NLDAS-2 forcing data are at a 0.125° spatial resolution (roughly 12 km) and are available from 1 January 1979 to within 5 days of real time, a latency that may be reduced by combination of NLDAS-2 reanalysis with other, real-time analysis data sources (as in Part II). NLDAS-2 data are converted for use in the ASCE Standardized Reference ET Equation [Eq. (1)] using procedures detailed in Allen et al. (2005).

c. Evaluation approach

Four example basins are drawn from across CONUS's hydroclimatic spectrum (see Table 1 and Fig. 2): they differ in size, land cover, topography, and hydroclimate (from the predominantly energy-limited Allegheny River basin to the predominantly water-limited upper Colorado basin). The basin of the Allegheny River at Natrona, Pennsylvania (hereafter the "Allegheny basin"), has a humid continental climate with warm summers and cold winters (with over 1000 mm of snow). The basin of the Current River at Doniphan, Missouri (Current basin), is a primarily forested basin (78% by area) located in the agricultural Midwest, with a mean elevation of 300 m (Slack and Landwehr 1992) and a rainfall-dominated hydroclimate. The basin of the Russian River near Ukiah, California (Russian basin), has a Mediterranean climate with a distinct wet, winter season (80% of Prcp falls from November to March) and a hot, dry summer season. The basin of the Colorado River near Cisco, Utah (upper Colorado basin), is the largest and most spatially heterogeneous—typified by the high mountain ranges and sparse forests of the central Rocky Mountains, intervening rangeland, and occasional irrigated valleys—and has a snowmelt-dominated hydroclimate.

Data sources used for the comparison of E_0 against other basinwide fluxes and states are as follows: Prcp is extracted from the Parameter-Elevation Regressions on Independent Slopes Model (PRISM; Daly et al. 1994),
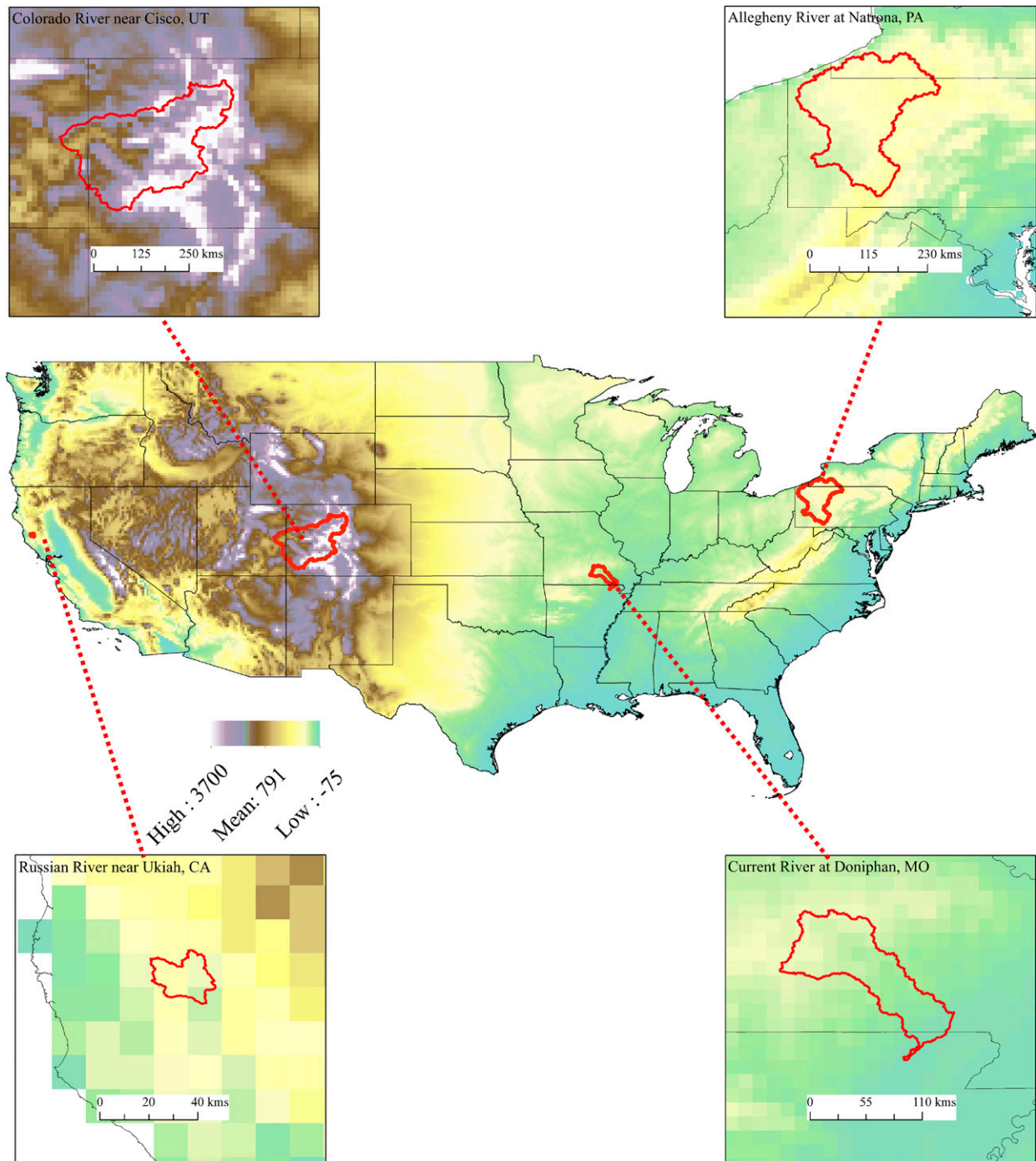
FIG. 2. Location of the four basins used in this study, including NLDAS-2 elevation (m) above mean sea level.

RO data are from U.S. Geological Survey (USGS) data sources for hydrologically undisturbed basins listed in the Hydro-Climatic Data Network (Slack and Landwehr 1992), SM is available from the Variable Infiltration Capacity model (Liang et al. 1994) driven by NLDAS-2 forcings, and ET is from the Atmosphere–Land Exchange Inverse (ALEXI) surface energy balance algorithm model (Anderson et al. 1997).

For comparison with other drought indicators, we evaluate EDDI against the USDM, the leading operational drought-monitoring tool in the United States. The USDM is a composite drought indicator, published

weekly since 4 January 2000, by the National Drought Mitigation Center (http://droughtmonitor.unl.edu/) at the University of Nebraska–Lincoln. The USDM attempts to capture drought intensity, duration, spatial extent, and probability of occurrence, while identifying specific drought types (e.g., hydrologic vs agricultural). The USDM has long been influential across sectors and stakeholder types with respect to drought-response decision-making. Though not completely objective (it incorporates local expert knowledge), it currently serves as the best available benchmark for much drought-monitoring research.

4. Results

The following results demonstrate the underlying principles of EDDI and its relevance to drought. Accordingly, section 4a demonstrates the multiscalar, early warning utility of EDDI and offers suggestions on selecting an aggregation window, section 4b examines how the drivers of E_0 perform under flash drought, and section 4c illustrates the complementary and parallel interactions of ET and E_0 and the linkage of E_0 to the water balance within the context of these two interactions.

a. EDDI as a multiscalar, leading indicator

Similar to the SPI and other drought indices, EDDI is formulated as a multiscalar metric from which specific time-aggregated versions can be selected (e.g., from 1 week to 12 months or longer). Depending on hydroclimate, certain aggregations can provide a leading indication of drought development. Figure 3 illustrates this behavior for the four example basins by examining the time evolution of different time scales of EDDI compared to the USDM analysis over a period of 15 years. By design, the shorter-range EDDIs fluctuate rapidly while the longer-range EDDIs change gradually; the spread of the various EDDI traces arises from drying and wetting responses on different time scales. The figures illustrate that the fast-responding, short-time-scale EDDIs offer the most potential for depicting an impending change in drought condition, but are unreliable for characterizing the severity of an established drought. Shorter-period EDDIs may be particularly useful in smaller basins that respond rapidly to intense, high-frequency events. Examples of this are evident in the Current and Russian basins (Figs. 3b,c). In the Russian basin, an instance of short-term abatement and rapid reemergence of drought in the winter and spring of 2007/08 is presaged by 1–12-weekly EDDI many months before the USDM: in fact, EDDI shows drought reemergence well before the USDM has even responded to the prior abatement. Further, the drought abatement

in the winter of 2014/15 (due to the landfall of an atmospheric river in Northern California) in the short-term EDDI signal leads the USDM by many weeks. As an example of the ongoing monitoring of long-term, sustained droughts, the longer-term EDDI mirrors the intense ongoing California drought from 2011 to the present. In the Current basin, both the short- and long-time-scale EDDI give early warning (with respect to the USDM) of the two most significant droughts—during 2011 and the flash drought in 2012 (see Fig. 5, described in greater detail below, and section 4b for more on this drought). For example, the longer-term EDDIs increase approximately 6 months in advance of the USDM's 2011 drought. Further, observe that while the USDM indicates a period of no drought between these two droughts, both long- and short-term EDDI remain elevated between them. Thus, despite the USDM reporting that the 2011 drought has ended, the extra information contained in EDDI shows that at no time scales have evaporative conditions returned to normal, setting the stage for a rapid reemergence of drought in 2012.

Longer-time-scale EDDIs may more usefully capture the slower response of larger basins and/or those with significant snowmelt-lagged hydroclimates, such as the Allegheny basin (Fig. 3a) and the upper Colorado basin (Fig. 3d). In the Allegheny basin, the USDM reports much shorter droughts than in the western basins. The drought of 2001–02 appears in the EDDI signal but without any clear warning provided by EDDI (even at shorter time scales). The nondrought period from the summer of 2003 to the spring of 2005 is reflected in EDDI, but thereafter, longer-term EDDI appears to indicate drought where none is reported by USDM. In the upper Colorado basin (Fig. 3d), short-range EDDIs appear to have little relationship to drought variations, indicating a mismatch between these time scales and the basin's spatial scale and/or snowmelt-dominated hydroclimate. On the other hand, longer-time-scale EDDIs appear to offer information that is as yet missing from the USDM, including early warning: not only do many of the monthly EDDIs start increasing well in advance of the USDM registering drought onset (see 2001, 2007, 2008, 2010, and 2015), but they remain elevated both in interdrought periods (as indicated by the USDM; see 2011), in ongoing droughts, and in periods of increasing severity (see 2002, 2005, and 2012) and abatement (see 2013–14).

Overall, selecting the aggregation period to maximize leading or ongoing information about drought depends on the hydroclimate of the region of interest and on users' sector-specific needs. The correlation analysis of Fig. 4 provides a useful diagnostic approach for optimizing aggregation period. The surface shows the
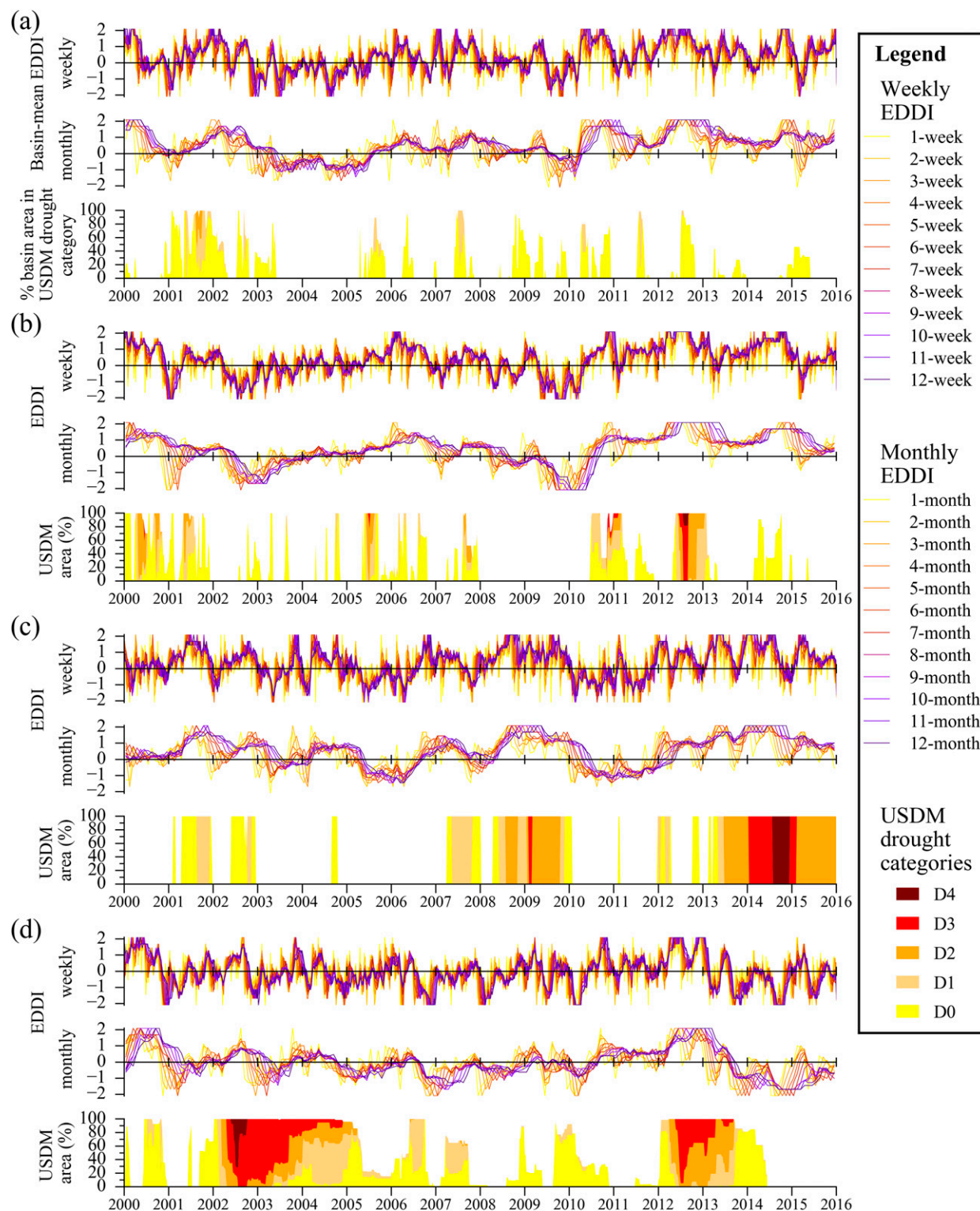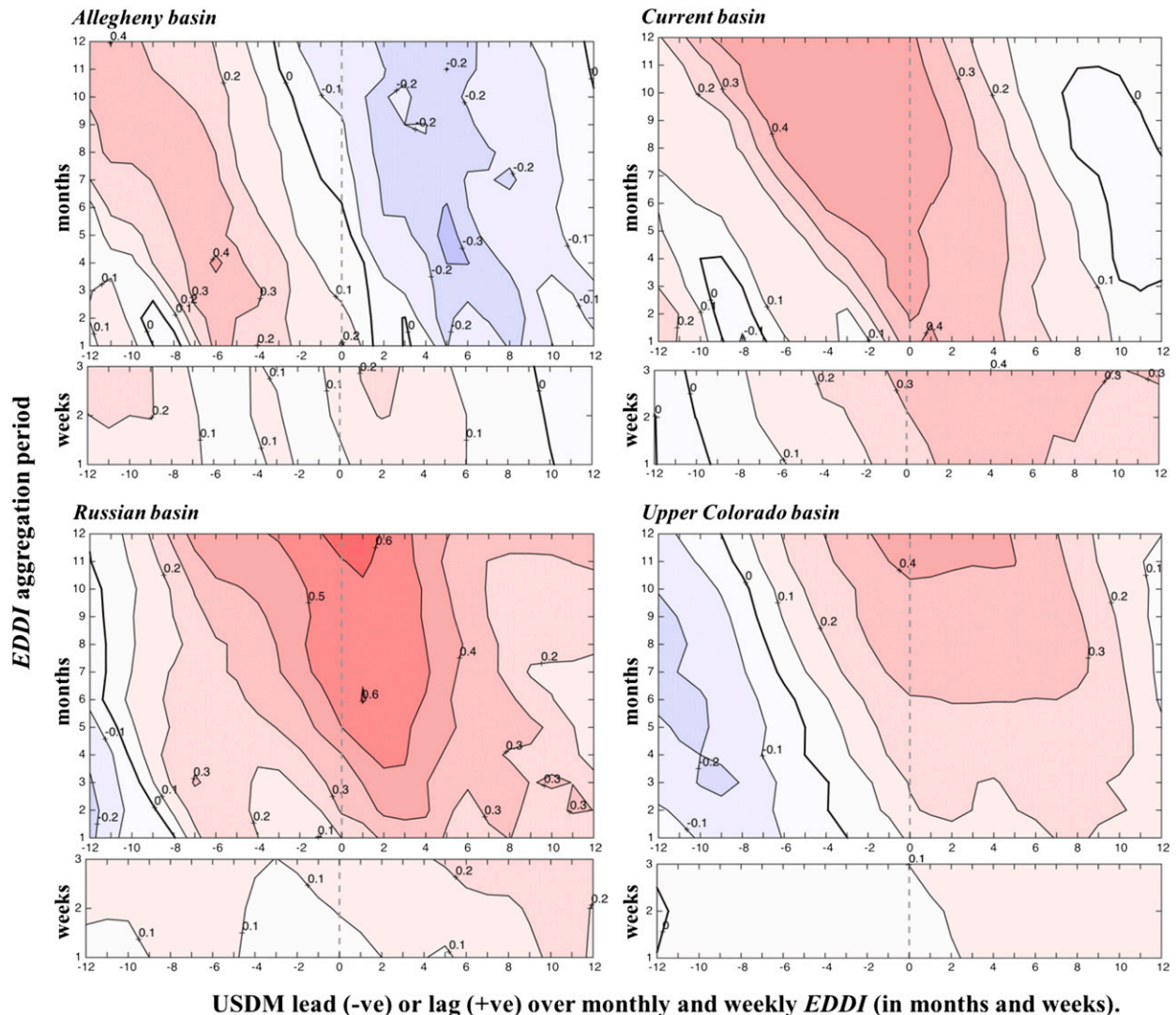
FIG. 3. Basinwide time variations of multiweekly and multimonthly EDDI and weekly USDM for the entire USDM period (from 4 Jan 2000 to the present) across (a) the Allegheny basin, (b) the Current basin, (c) the Russian basin, and (d) the upper Colorado basin. Within each panel, shown from top to bottom are 1–12-weekly EDDI, 1–12-monthly EDDI, and the weekly time series of USDM.

FIG. 4. Correlations between river basin spatial means of USDM and EDDI. EDDI varies from 1- to 3-week and 1- to 12-month aggregation periods shown on the ordinate axes, with lead (lag) times between USDM and EDDI of up to ±12 weeks and months (for weekly and monthly EDDI, respectively) shown on the abscissae. Correlations are indicated by color: red is positive and blue is negative.

correlation coefficient r between time series of EDDI and USDM for aggregation period lengths varying from 1 to 12 weeks and 1 to 12 months, for various lags (EDDI lags USDM) and lead times (EDDI leads USDM) between the two time series, for four hydroclimatically different basins. To the right of the vertical dashed line at 0 lag, EDDI leads USDM.

The differences between the correlation surfaces between basins are most likely due to their hydroclimates. For example, in the upper Colorado basin, the 10–12-month optimal aggregation period yields a lead time over the USDM of up to 5 months, while there is little association between EDDI and USDM at the shorter 1–3-weekly aggregation periods. These long lead times and

aggregation periods are likely due to the significant lagged influence of snowpack on river flow anomalies. Dry climate anomalies in the snow accumulation period are reflected in the EDDI signal but may only be reflected in the USDM signal in the subsequent growing or irrigation season. In contrast, in the Russian basin, which has little to no snow, there is a lobe of elevated information content ($r > 0.5$) that stretches down to short-term EDDI at about a 2–3-month aggregation period, where it leads the USDM signal by upward of 4 months.

The Allegheny basin provides a counterexample, in which EDDI does not appear to be positively correlated to USDM at 1–12-monthly time scales with any useful

lead time. Positive correlation of EDDI with USDM with lead time is only apparent in the shorter 1–3-week EDDI. This appears to indicate that EDDI may not be an appropriate drought early warning metric in this region. Potential causes for the apparent weak response of EDDI to drought here are further discussed in relation to Fig. 6 (described in greater detail below). Nonetheless, in comparing EDDI to SPI and the standardized soil moisture index, Part II shows that EDDI remains a potentially useful indicator for flash drought and growing-season drought monitoring in this region.

A distinct characteristic of the correlation surfaces is that, at longer aggregation periods, EDDI appears to lag the USDM—observe the "leaning" of the correlation space toward the left at longer EDDI aggregation periods. This is most likely because of the nature of the USDM, which is a blend of nonphysical inputs (such as expert local knowledge) and physical inputs at a variety of time scales. Many of these physical inputs will be at shorter time scales than long-term EDDI and will therefore be more reactive to short-term transient meteorological and/or radiative forcings than EDDI at these scales, which react more slowly because of its long memory. This hypothesis bears further investigation, but overall, the shape of the correlation surfaces do appear to favor EDDI as a leading indicator of the USDM at EDDI aggregations periods below a threshold that depends on the basin.

b. Decomposing drought evaporative demand dynamics

It is instructive to explore how variations of drivers of E_0—T_{air}, q, R_d, and U—relate to E_0 and EDDI under varying conditions of drought and to decompose and attribute the evaporative signature of drought to its meteorological and radiative drivers. Variations in E_0 accumulate as a function of both the anomalies (hereafter denoted by Δ, e.g., ΔE_0 is the anomaly in E_0) in these driving variables and the sensitivities of E_0 to them (e.g., $\partial E_0/\partial q$), as follows:

$$\Delta E_0 = \frac{\partial E_0}{\partial T_{air}}\Delta T_{air} + \frac{\partial E_0}{\partial q}\Delta q + \frac{\partial E_0}{\partial R_d}\Delta R_d + \frac{\partial E_0}{\partial U}\Delta U. \quad (5)$$

Each term on the right-hand side represents the contribution to anomalies in E_0 by each driving variable [analytical expressions of the sensitivities are provided and mapped across CONUS in Hobbins (2016)]. Which terms dominate E_0 variability has been shown across CONUS and seasons for synthetic pan evaporation in Hobbins et al. (2012) and for ASCE reference ET in Hobbins (2016). Clearly, these variations combine to

determine the variability of the evaporative drivers and responses of drought. These terms give insight into the meteorological factors contributing to the flash drought and into whether the E_0 reanalysis (and therefore EDDI) provides advance warning. In Fig. 5a, for example, the E_0 signal of a period of flash drought is related to its driving variables using Eq. (5) at a 2-week aggregation period for the calendar year 2012 in the Current basin. The drought period is portrayed by the USDM (Fig. 5b) starting in May but rapidly deepening through June to peak intensity in August before abating. Figure 5a (top) tracks the 2-week ΔE_0 and the contributions to ΔE_0 of each of the four drivers in millimeter depths accumulated across a 2-week period that steps daily. In the remainder of Fig. 5a, daily E_0 and its four drivers (T_{air}, q, R_d, and U) are also plotted with their 30-yr (1981–2010) daily means for comparison. Drivers T_{air} and q make the largest contributions to ΔE_0: with the majority of T_{air} contributions to ΔE_0 being positive, and of q being negative until late May and positive thereafter. The contribution from high U is small by comparison (though always positive) until early June, when it climbs to 10–20 mm until late October, coinciding with the intensification of drought conditions. This is confirmed by the daily U trace, which is generally above normal from June to September. Although R_d is often above normal, the minimal sensitivity of E_0 to R_d in this region (Hobbins 2016) results in it making little contribution to ΔE_0 across the year.

As the year starts, the contribution from the above-normal T_{air} is largely mediated by above-normal q, leaving ΔE_0 near zero after February. In March and April, both T_{air} and q spike well above normal, with q making a (negative) contribution of almost -60 mm to ΔE_0 but T_{air} making a positive contribution of 60 mm and combining with U contributions to steadily increase ΔE_0 (and so increase EDDI). In late May, Δq switches signs and combines with the still-positive ΔT_{air}, leading ΔE_0 to climb rapidly to a 2-week surplus of 80 mm in early July. This is recorded by the USDM as a "flash drought" or a sudden increase in USDM drought category across the basin. As shown in Fig. 5b, the event was to some extent foreshadowed in the previous months by EDDI, which reached its maximum value for many time scales in the spring. EDDI goes on to provide early warning of the peak of the drought, with short-term EDDI peaking approximately 1 month before the USDM reported maximum drought intensity (category D4, or "exceptional drought").

The rapid return of E_0 to near-normal conditions in late July is driven by a rapid return to near-normal T_{air} and q combined with a sudden negative ΔU. However, these conditions last for only a few weeks before the
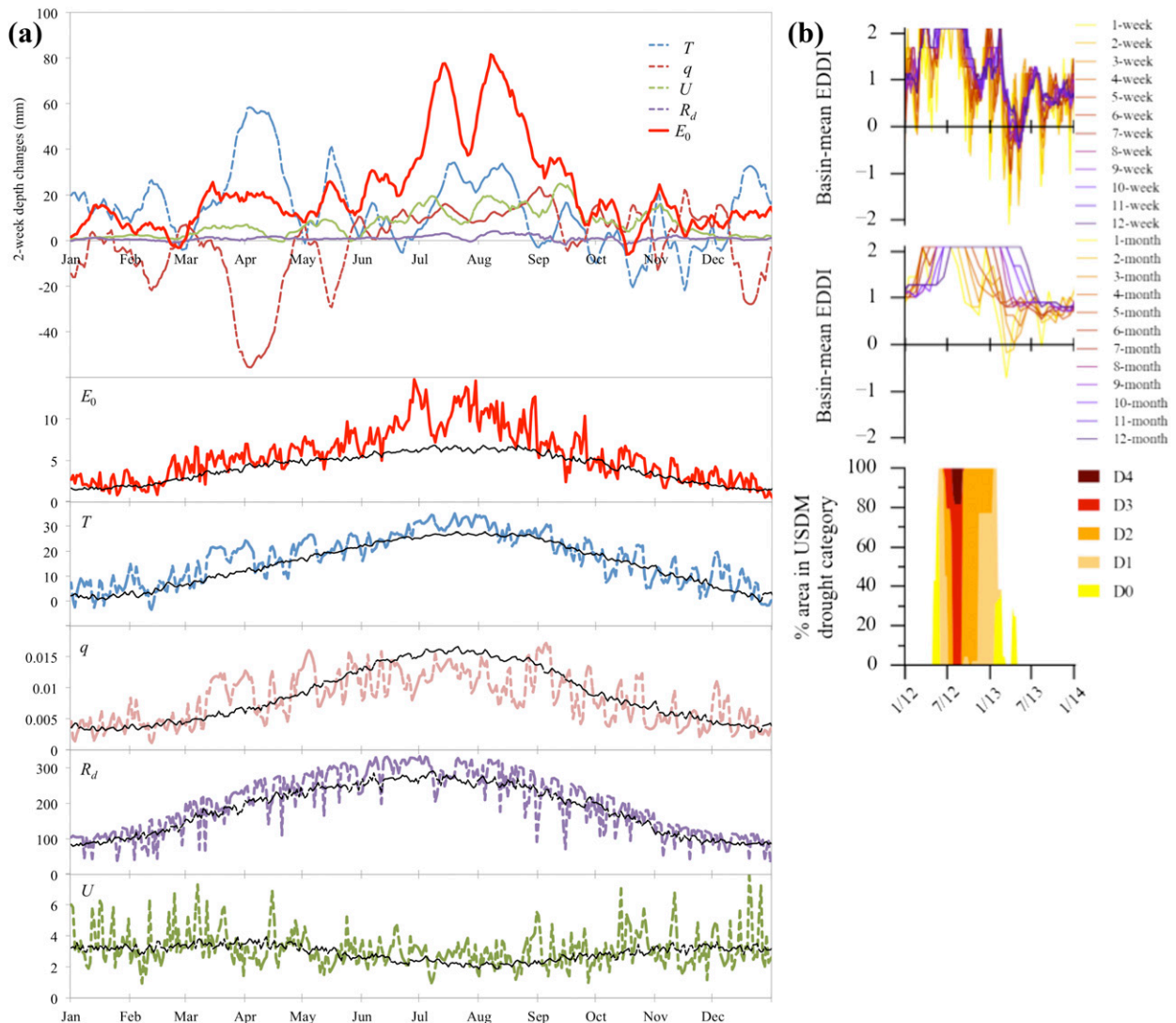
FIG. 5. Example of time variations of ΔE_0 and its drivers under a flash drought during the spring and summer of 2012, in the Current basin. (a) Two-week time series of ΔE_0 (mm) and each driver's contributions to ΔE_0 (mm) (top); below are daily time series of E_0 (mm day^{-1}), T_{air} (°C), q (kg kg^{-1}), R_d (W m^{-2}), and U (m s^{-1}), with daily climatological (1981–2010) mean values in black. (b) The time series of drought monitors across the basin are shown for a 2-yr period 2012–13 including the flash drought: 1–12-weekly EDDI in (top), 1–12-monthly EDDI in (middle), and weekly USDM plotted as percentage of basin in each USDM drought category in (bottom) (the full time series is shown in Fig. 3b).

drivers return to severe drought conditions and the E_0 surplus peaks again in early August, thereafter extending positively into the fall. In late October, all drivers have returned to near-normal conditions and, as indicated by short-term EDDI, the drought has significantly abated; it is eliminated early in the following year. Considering these results, it is possible that E_0 and 2-week EDDI presaged drought in early March, yet it is unclear whether the high EDDI conditions in the spring were a necessary table setting for the descent into drought later. Certainly variation in

the drivers of EDDI just before and during the event were consistent with drought, and the physical framework for decomposing E_0 provides insight into proximate factors influencing the drought. Part II (their Figs. 6 and 7) also examines this period of drought in the region by conducting a nonexplicit sensitivity analysis to establish the effects of each of the drivers on EDDI (as opposed to the E_0 examined here); they demonstrate the role of the advective portion of E_0 in driving flash droughts and EDDI's ability to provide drought early warning.
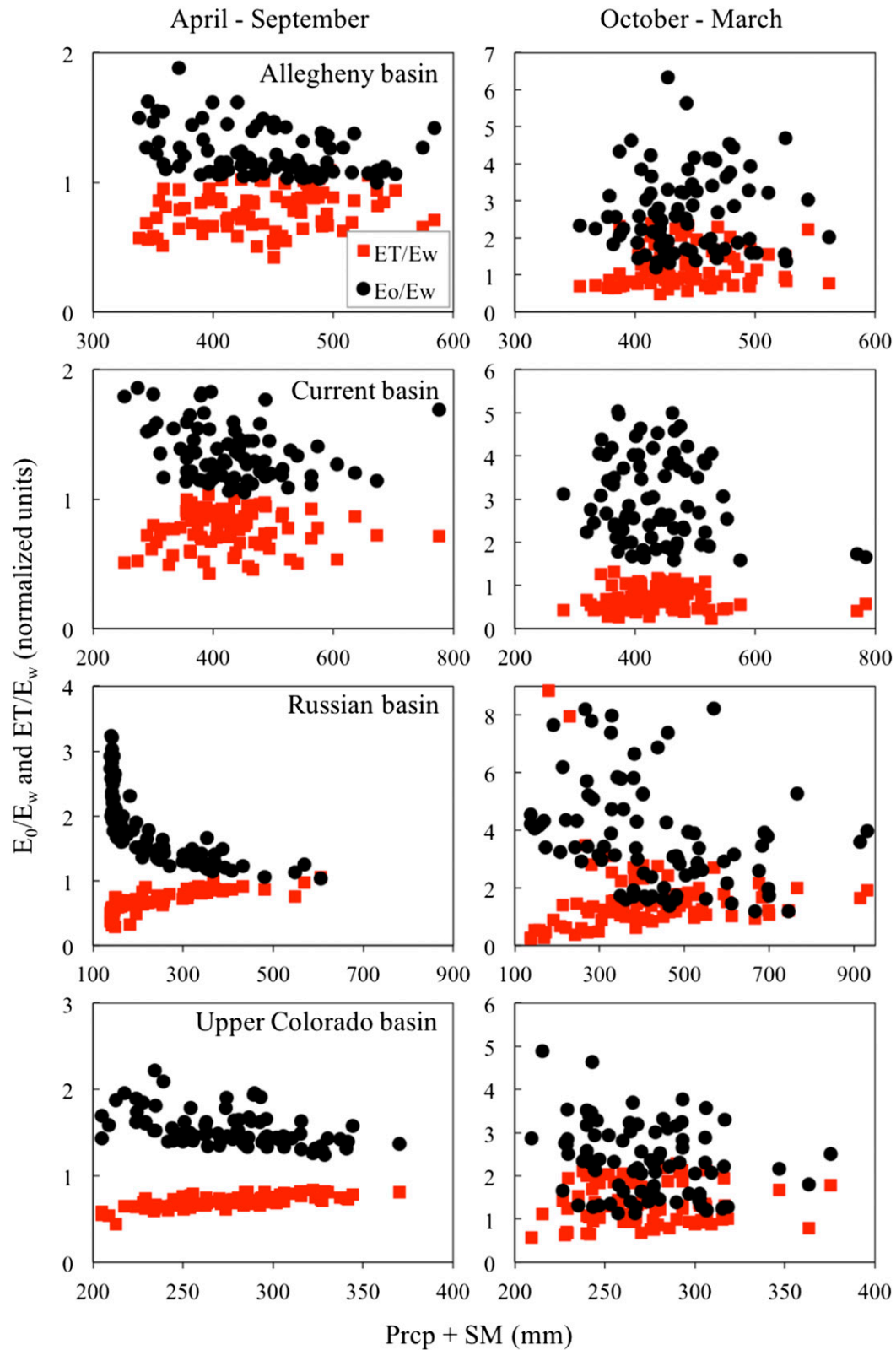
FIG. 6. The monthly ET–E_0 relationships in the four example basins across (left) the warm, dry April–September period and (right) the cool, wet October–March period. Data are from 2000 to 2013.
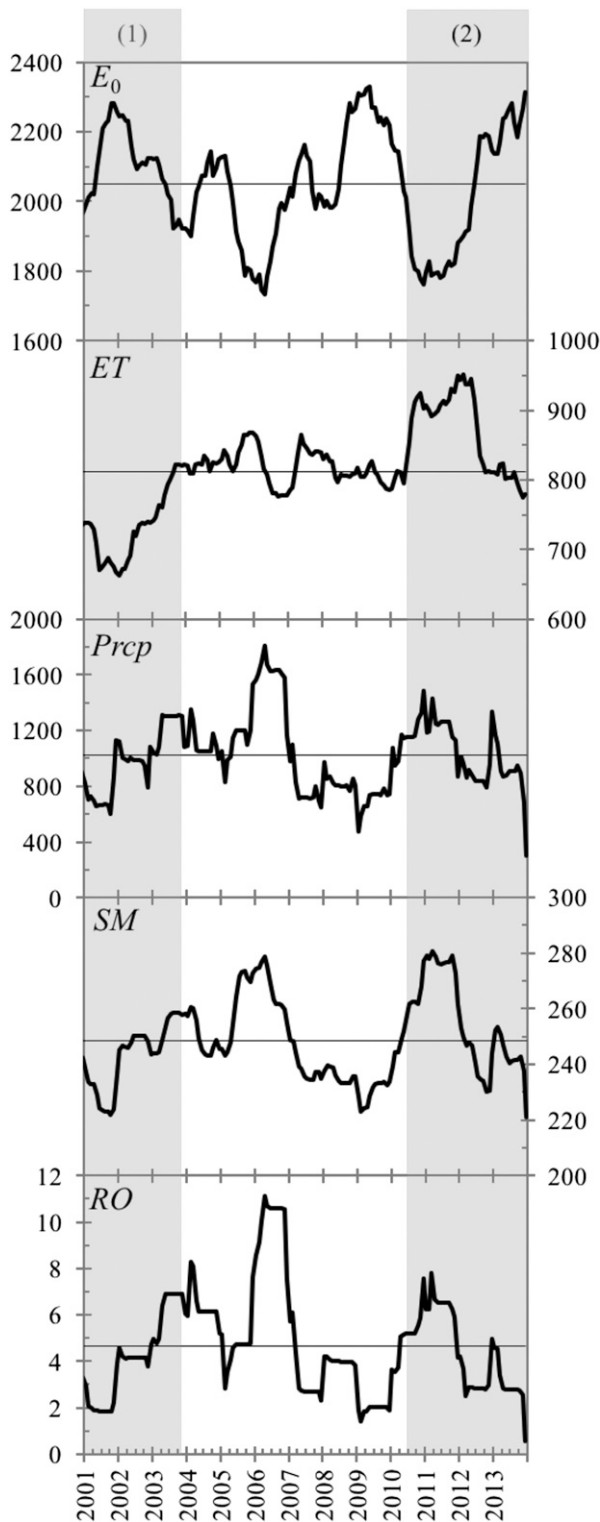
FIG. 7. Linkages between water balance components demonstrating basinwide variations in E_0, ET, Prcp, SM, and RO for the Russian basin from January 2010 to December 2013, stepping monthly, with each series mean shown as a horizontal line. Variables E_0, ET, Prcp, and SM are basinwide-mean annual depths (mm), and RO is the 12-month mean streamflow measured at the basin outlet (m³ s⁻¹). Numbered shaded periods denote periods discussed in the text.

c. Complementary and parallel evaporative dynamics

The drought-related behaviors of E_0, ET, and other hydrologic states, fluxes and E_0 drivers are illustrated using all four example basins in order to represent a variety of hydrologic responses to drought resulting from their differences in hydroclimate, size, topography, and vegetation (see Table 1).

Figure 6 portrays the two ET–E_0 relations previously described—parallel and complementary—and shows the extent to which complementarity holds in the four test basins. Variables ET and E_0 are normalized by E_w from the Priestley–Taylor equation (Priestley and Taylor 1972) and are shown as a function of water availability (represented by monthly Prcp plus mean monthly SM). Though not nondimensional [which is preferred by Kahler and Brutsaert (2006)], the complementarity patterns are usefully expressed.

In general, the relationship holds well in the Current, upper Colorado, and Russian basins—particularly in the latter—but poorly in the Allegheny basin. Following, we contrast the two extremes of response: the Russian and Allegheny basins. For the Russian basin, E_0 declines with increasing Prcp in both wet and dry seasons, indicating the effects of extra cloudiness, lower irradiance, and sensible heating of the dynamic boundary layer from the surface, in favor of higher latent heat flux (so higher ET). The complementarity is particularly strong during the drier, water-limited summer months, when ET declines while E_0 increases with energy availability. In contrast, water is available for ET during the high-Prcp winter periods (January–May), leaving ET energy limited and increasing in line with increasing energy availability (and hence with E_0). Thus, both parallel (November–March) and complementary (May–September) ET–E_0 relations occur within the year. At annual time scales (not shown) these moisture and energy differences average out and the overall ET–E_0 complementarity becomes more evident.

Across the Allegheny basin, on the other hand, ET–E_0 complementarity is not evident in either wet or dry periods. Pennsylvania has been identified as a region where high SM exerts little control on ET because of the prevailing energy-limiting conditions (Koster et al. 2009). A weaker coupling between the land surface and the atmosphere at shorter time scales may be due to various factors: greater water storage in heavily forested regions mediating the meteorological and radiative variations that drive E_0 variability, even at seasonal time scales, leaving moisture available for sustained ET long after E_0 conditions might indicate otherwise; transpiration shutting down in the winter, leaving ET to originate exclusively from soil, snow, and surface water; and that

over heterogeneous topography (with elevated terrain shadowing) ALEXI estimates ET with higher errors, and from snow, not at all.

Figure 7 demonstrates as time series the 14-yr development of various water balance components for the Russian basin. Data are accumulated (or averaged, for SM) across a 12-month moving window that steps monthly. The parallel responses of SM and RO to Prcp are immediately clear. To a lesser degree, ET also tracks Prcp well, increasing during the highest Prcp periods of 2002–07 and 2010–12. However, ET does not only vary in response to the availability of water (from Prcp and SM) but also to the availability of energy (as reflected in E_0). During water-limited periods when there is enough energy available to evaporate all the available moisture, ET and E_0 vary in a complementary fashion. During energy-limited periods when there is enough moisture to evaporate at the prevailing maximal energy conditions, ET and E_0 vary in a parallel fashion. The two numbered shaded periods provide educative examples of these varying parallel and complementary ET$-E_0$ relations, as follows:

1) The basin starts with negative ΔPrcp and ΔSM and is thus water limited relative to mean conditions. This causes complementary relations between ET and E_0, with ΔET and ΔE_0 being of opposite sign. As Prcp increases throughout the period, so too does water-limited ET, while E_0 declines—still varying in complementary directions.

2) The basin starts in an energy-limited condition, due to positive ΔPrcp and ΔSM resulting in elevated water availability and leading to parallel ET$-E_0$ relations as increasing E_0 drives increasing ET. Then, in the second half of the period, declining Prcp and SM decrease water availability and ET$-E_0$ relations turn complementary with rapidly decreasing ET driving increasing E_0.

5. Discussion and conclusions

a. Summary

This paper presents the physical basis and utility of a drought index based on E_0 alone—the Evaporative Demand Drought Index (EDDI). Part II verifies the performance of EDDI against other commonly used drought indices across CONUS. The key rationale for EDDI is that E_0 reflects drying anomalies through complementary and parallel feedbacks with ET (among other water balance components) that implicitly encode moisture availability. In case studies in several basins, this is manifest as a robust signal in E_0 that responds to dry anomalies across time scales. We demonstrate the

attributive utility of E_0 as a drought indicator by explicitly decomposing the evaporative drivers of drought dynamics for a flash drought. We illustrate the time evolution and multiscalar properties of EDDI in time series comparisons to established drought monitors across four basins and demonstrate EDDI's potential to serve as a leading indicator of drought.

b. Strengths of EDDI

The primary strengths of EDDI are its early warning capabilities, its independence from Prcp- and SM-based metrics, its derivation from reanalyses, and its utility in the attribution of drought dynamics.

EDDI has clearly demonstrated early warning of drought relative to the USDM in three of the four basins examined here: that they are the three most water-limited basins is likely due to the strength of complementarity typical in those hydroclimates. Early warning is a long-sought-after goal in drought monitoring, as it opens or extends a decision window to water and land managers charged with preserving valuable natural and economic resources under hydroclimatic extremes, a particular challenge in the water-limited regions where economic and operational margins are finer.

As EDDI is derived from an E_0 that is itself derived from reanalyses, coverage is complete in both space and time and data are available with low latency. Further, as E_0 estimation is independent of SM and Prcp, EDDI avoids issues relating to highly parameterized LSMs and to Prcp uncertainties that may be significant in poorly sampled, orographically influenced, or highly convective regions. While the ESI is also independent of Prcp, that EDDI has no gap-filling requirements is a relative strength.

A key advantage that provides users additional explanatory information as to the origins of drought is that using E_0 as an underlying metric of drought permits explicit attribution of drought mechanisms into relative forcings from its meteorological and radiative drivers. Such a decomposition gives a more in-depth understanding of current conditions relative to long-term means. This is an important advance as one can now explain why other drought monitors, such as the USDM, may be showing intensifying or mediating drought, by separating E_0 variations into their widely measured drivers (T_{air}, R_d, q, and U).

c. Take-home messages for potential users

EDDI converts E_0 into a drought index in an easy-to-compute manner, though a significant caveat is that only physically based E_0 measures [such as those based on Penman–Monteith (Monteith 1965) or Penman (1948)] will encode the necessary physical interactions of E_0

with the hydrologic cycle and meteorological forcings: though their simplicity often makes them attractive, T_{air}-based E_0 parameterizations must not be used.

EDDI detects both flash and sustained droughts in a manner that is consistent with the USDM and other SM- and ET-based drought metrics in both pattern and intensity. Though not shown, E_0 correlates strongly with SM, which underlines both its role as a predictor of meteorological variability and moisture availability within the agricultural sector and its potential as a monitor of agricultural drought. The combination of the E_0 rise in response to both fast-developing and sustained droughts often weeks to months prior to the USDM and using driving variables' with a low latency—about 5 days for our NLDAS-2-based E_0—suggests EDDI's utility in real-time drought monitoring and as a robust leading indicator of drought.

EDDI's multiscalar properties permit different drought-monitoring functionalities as the signals of various drying dynamics are evident at different time scales: short-term EDDI may serve as an early warning signal of drought, especially in agricultural areas; long-term EDDI may be useful for water-limited hydrologic drought monitoring. Operational time frames will vary with hydroclimate, scale, and sector, but their optimization is straightforward. Early adopters of the index report using a mix of time scales (N. Doesken, Colorado State Climatologist, 2015, personal communication).

Based on these example basins, there may be regions where EDDI does not offer as much early warning capability as it does in more water-limited basins, or basins where the complementarity between ET and E_0 is more pronounced. Users in these regions may be limited as to the optimal time scale for EDDI. Clearly more work is needed on this question. This is addressed in more detail in Part II.

Finally, while drought cannot be determined by a single index alone, EDDI can act as a validation of SM- and Prcp-based metrics and can confirm or provide early indication that dynamics that may lead to drought are underway. EDDI's higher propensity for false alarms is not indicative of deficiencies in the method, but rather that not all high-demand episodes will eventuate into "on the ground" impacts. For example, when EDDI indicates developing drought that is then supported by ESI (i.e., a signal of stressed vegetation), this may be a result of a drying evolution that precedes indicators based on vegetation health; this may then give some early confidence to drought decision-makers. In this way, E_0- and ET-based drought indices complement each other, with E_0 demonstrating the potential for drought onset due to meteorological and radiative forcing, while the actual susceptibility of different systems to these potential events is conveyed by ET. We

conclude that EDDI is a useful complement to existing indices, where it can contribute both ongoing monitoring and early warning components to the convergence of evidence approach used in drought analysis.

d. Caveat for climate-scale EDDI

The use of EDDI in long-term or climate-scale drought analyses is subject to a strong caveat. Using reference ET for E_0 is reasonable across time scales of individual droughts or across a multidecadal climatology—periods during which atmospheric CO_2 varies little. However, CO_2 changes substantially at climate scales, leading models in phase 5 of the Coupled Model Intercomparison Project (CMIP5) to project an annual increase in reference ET of ~230 mm for 2099 relative to 1999 (Roderick et al. 2015). All else equal, and without changes in the climatology period, this would lead EDDI to imply increasing aridity in a warming climate. However, the interpretation of increasing reference ET in the long term is by no means settled, with only recent work resolving these projections with the geologic record (Roderick et al. 2015). Only with due care given to the selection of climatology period (too long and the trend dominates; too short and drought-scale variability cannot be characterized with confidence) can E_0-based metrics like EDDI be deemed suitable drought metrics for climate-scale analyses.

e. Future research

This paper suggests many directions for future research. Beyond EDDI itself, improvements to the USDM with respect to its treatment of evaporative demand—currently limited to roles in estimating ET from LSMs or physics-poor implementations of E_0 hidden inside other drought tools—could accrue by inclusion of the NLDAS-2-forced E_0 reanalysis (i.e., the E_0 underpinning EDDI) as a driver of LSMs and drought indices. Indeed, on time scales pertaining to both ongoing and flash droughts, using a physically based observed E_0 driver that is spatially distributed, well-calibrated, physically representative, and available on a daily basis with limited latency will enhance characterization of the evaporative dynamics of ongoing drought, and the resulting EDDI can provide an important perspective that is as yet missing. Further work will evaluate EDDI's potential as an early warning indicator of drought, perhaps as a complement to the ESI. As a stand-alone metric, EDDI may identify potential drought onsets by observing high-frequency E_0 surpluses using a small aggregation period filter and then verify these using a longer aggregation period filter. The strong physical linkage that E_0 provides between weather-scale events and forest physiology suggests the use of EDDI in

wildfire prediction: indeed, it is currently in experimental use by the U.S. Forest Service Southern Research Station in its seasonal forecasts of large fires on U.S. lands and their suppression costs (Ham et al. 2014). Forecasts of E_0 itself—currently produced at the daily and weekly time scales by the National Weather Service (Snell et al. 2013) and under investigation at the seasonal time scale (McEvoy et al. 2016b)—suggest the possibility of drought forecasting from the evaporative perspective. Overall, explicating the role of E_0 in drought occurrence will deepen our understanding of water and energy cycle phenomena, thereby improving operational water management, drought monitoring and prediction, and decision-making in water-dependent sectors.

REFERENCES

Abramowitz, M., and I. A. Stegun, 1965: *Handbook of Mathematical Functions, with Formulas, Graphs, and Mathematical Tables.* Dover Publications, 1046 pp.

Allen, R. G., I. A. Walter, R. Elliott, T. Howell, D. Itenfisu, and M. Jensen, 2005: The ASCE standardized reference evapotranspiration equation. Rep. 0-7844-0805-X, 59 pp. [Available online at http://www.kimberly.uidaho.edu/water/asceewri/ascestzdetmain2005.pdf.]

Anderson, M. C., J. M. Norman, G. R. Diak, W. P. Kustas, and J. R. Mecikalski, 1997: A two-source time-integrated model for estimating surface fluxes using thermal infrared remote sensing. *Remote Sens. Environ.*, **60**, 195–216, doi:10.1016/S0034-4257(96)00215-5.

——, ——, J. R. Mecikalski, J. A. Otkin, and W. P. Kustas, 2007: A climatological study of evapotranspiration and moisture stress across the continental United States based on thermal remote sensing: 2. Surface moisture climatology. *J. Geophys. Res.*, **112**, D11112, doi:10.1029/2006JD007507.

Bouchet, R. J., 1963: Évapotranspiration réelle et potentielle, signification climatique. *IAHS Publ.*, **62**, 134–142.

Budyko, M. I., 1974: *Climate and Life.* International Geophysics Series, Vol. 18, Academic Press, 508 pp.

Dai, A., K. E. Trenberth, and T. Qian, 2004: A global dataset of Palmer drought severity index for 1870–2002: Relationship with soil moisture and effects of surface warming. *J. Hydrometeor.*, **5**, 1117–1130, doi:10.1175/JHM-386.1.

Daly, C., R. P. Neilson, and D. L. Phillips, 1994: A statistical–topographic model for mapping climatological precipitation over mountainous terrain. *J. Appl. Meteor.*, **33**, 140–158, doi:10.1175/1520-0450(1994)033<0140:ASTMFM>2.0.CO;2.

Farahmand, A., and A. AghaKouchak, 2015: A generalized framework for deriving nonparametric standardized indicators. *Adv. Water Resour.*, **76**, 140–145, doi:10.1016/j.advwatres.2014.11.012.

Guttman, N. B., 1999: Accepting the Standardized Precipitation Index: A calculation algorithm. *J. Amer. Water Resour. Assoc.*, **35**, 311–322, doi:10.1111/j.1752-1688.1999.tb03592.x.

Ham, C., M. T. Hobbins, K. L. Abt, and J. P. Prestemon, 2014: Using the Evaporative Demand Drought Index and the Palmer drought severity index to forecast the number of large wildland fires on federal lands. *Large Wildland Fires Conf.*, Missoula, MT, Association for Fire Ecology and the International Association of Wildland Fire. [Available online at http://largefireconference.org/wp-content/uploads/2013/06/Oral-Presentation-Abstracts-V4.pdf.]

Hargreaves, G. H., and Z. A. Samani, 1985: Reference crop evapotranspiration from temperature. *Appl. Eng. Agric.*, **1**, 96–99, doi:10.13031/2013.26773.

Hobbins, M. T., 2016: The variability of ASCE standardized reference evapotranspiration: A rigorous, CONUS-wide decomposition and attribution. *Trans. ASABE*, **59**, 561–576, doi:10.13031/trans.59.10975.

——, J. A. Ramírez, and T. C. Brown, 2004: Trends in pan evaporation and actual evaporation across the conterminous U.S.: Paradoxical or complementary? *Geophys. Res. Lett.*, **31**, L13503, doi:10.1029/2004GL019846.

——, A. Dai, M. L. Roderick, and G. D. Farquhar, 2008: Revisiting the parameterization of potential evaporation as a driver of long-term water balance trends. *Geophys. Res. Lett.*, **35**, L12403, doi:10.1029/2008GL033840.

——, A. W. Wood, D. Streubel, and K. Werner, 2012: What drives the variability of evaporative demand across the conterminous United States? *J. Hydrometeor.*, **13**, 1195–1214, doi:10.1175/JHM-D-11-0101.1.

Huang, J., H. M. van den Dool, and K. P. Georgakakos, 1996: Analysis of model-calculated soil moisture over the United States (1931–1993) and applications to long-range temperature forecasts. *J. Climate*, **9**, 1350–1362, doi:10.1175/1520-0442(1996)009<1350:AOMCSM>2.0.CO;2.

Kahler, D. M., and W. Brutsaert, 2006: Complementary relationship between daily evaporation in the environment and pan evaporation. *Water Resour. Res.*, **42**, W05413, doi:10.1029/2005WR004541.

Koster, R. D., S. D. Schubert, and M. J. Suarez, 2009: Analyzing the concurrence of meteorological droughts and warm periods,

with implications for the determination of evaporative regime. *J. Climate*, **22**, 3331–3341, doi:10.1175/2008JCLI2718.1.

Liang, X., D. P. Lettenmaier, E. F. Wood, and S. J. Burges, 1994: A simple hydrologically based model of land surface water and energy fluxes for general circulation models. *J. Geophys. Res.*, **99**, 14 415–14 428, doi:10.1029/94JD00483.

McEvoy, D. J., J. L. Huntington, M. T. Hobbins, A. Wood, C. Morton, J. Verdin, M. Anderson, and C. Hain, 2016a: The Evaporative Demand Drought Index. Part II: CONUS-wide assessment against common drought indicators. *J. Hydrometeor.*, **17**, 1763–1779, doi:10.1175/JHM-D-15-0122.1.

——, ——, J. F. Mejia, and M. T. Hobbins, 2016b: Improved seasonal drought forecasts using reference evapotranspiration anomalies. *Geophys. Res. Lett.*, **43**, 377–385, doi:10.1002/2015GL067009.

McKee, T. B., N. J. Doesken, and J. Kleist, 1993: The relationship of drought frequency and duration to time scales. Preprints, *Eighth Conf. on Applied Climatology*, Anaheim, CA, Amer. Meteor. Soc., 179–184.

Mo, K. C., and D. P. Lettenmaier, 2015: Heat wave flash droughts in decline. *Geophys. Res. Lett.*, **42**, 2823–2829, doi:10.1002/2015GL064018.

Monteith, J. L., 1965: Evaporation and environment. *Symp. Soc. Exp. Biol.*, **19**, 205–234.

Mu, Q., M. Zhao, J. S. Kimball, N. G. McDowell, and S. W. Running, 2013: A remotely sensed global terrestrial drought severity index. *Bull. Amer. Meteor. Soc.*, **94**, 83–98, doi:10.1175/BAMS-D-11-00213.1.

Narasimhan, B., and R. Srinivasan, 2005: Development and evaluation of Soil Moisture Deficit Index (SMDI) and Evapotranspiration Deficit Index (ETDI) for agricultural drought monitoring. *Agric. For. Meteor.*, **133**, 69–88, doi:10.1016/j.agrformet.2005.07.012.

Palmer, W. C., 1965: Meteorological drought. U.S. Weather Bureau Research Paper 45, 58 pp. [Available online at http://www.ncdc.noaa.gov/temp-and-precip/drought/docs/palmer.pdf.]

Penman, H. L., 1948: Natural evaporation from open water, bare soil, and grass. *Proc. Roy. Soc. London*, **A193**, 120–145, doi:10.1098/rspa.1948.0037.

Priestley, C. H. B., and R. J. Taylor, 1972: On the assessment of surface heat flux and evaporation using large-scale parameters. *Mon. Wea. Rev.*, **100**, 81–92, doi:10.1175/1520-0493(1972)100<0081:OTAOSH>2.3.CO;2.

Quiring, S. M., 2009: Developing objective operational definitions for monitoring drought. *J. Appl. Meteor. Climatol.*, **48**, 1217–1229, doi:10.1175/2009JAMC2088.1.

Roderick, M. L., L. D. Rotstayn, G. D. Farquhar, and M. T. Hobbins, 2007: On the attribution of changing pan evaporation. *Geophys. Res. Lett.*, **34**, L17403, doi:10.1029/2007GL031166.

——, M. T. Hobbins, and G. D. Farquhar, 2009: Pan evaporation trends and the terrestrial water balance. I. Principles and observations. *Geogr. Compass*, **3**, 746–760, doi:10.1111/j.1749-8198.2008.00213.x.

——, P. Greve, and G. D. Farquhar, 2015: On the assessment of aridity with changes in atmospheric CO_2. *Water Resour. Res.*, **51**, 5450–5463, doi:10.1002/2015WR017031.

Sheffield, J., E. F. Wood, and M. L. Roderick, 2012: Little change in global drought over the past 60 years. *Nature*, **491**, 435–438, doi:10.1038/nature11575.

Slack, J. R., and J. M. Landwehr, 1992: Hydro-climatic Data Network (HCDN): A U.S. Geological Survey streamflow data set for the United States for the study of climate variations, 1974–1988. USGS Open-File Rep. 92-129, 193 pp. [Available online at http://pubs.usgs.gov/of/1992/ofr92-129/.]

Snell, H. D., C. K. Palmer, P. Krone-Davis, F. S. Melton, and M. T. Hobbins, 2013: National Weather Service forecast reference evapotranspiration. *2013 Fall Meeting*, San Francisco, CA, Amer. Geophys. Union, Abstract H21A-1012. [Available online at http://abstractsearch.agu.org/meetings/2013/FM/H21A-1012.html.]

Thornthwaite, C. W., 1948: An approach toward a rational classification of climate. *Geogr. Rev.*, **38**, 55–94, doi:10.2307/210739.

Vicente-Serrano, S. M., S. Beguería, and J. I. López-Moreno, 2010: A multiscalar drought index sensitive to global warming: The standardized precipitation evapotranspiration index. *J. Climate*, **23**, 1696–1718, doi:10.1175/2009JCLI2909.1.

——, J. I. López-Moreno, S. Beguería, J. Lorenzo-Lacruz, C. Azorin-Molina, and E. Morán-Tejeda, 2012: Accurate computation of a streamflow drought index. *J. Hydrol. Eng.*, **17**, 318–332, doi:10.1061/(ASCE)HE.1943-5584.0000433.

Wilks, D. S., 2011: Empirical distributions and exploratory data analysis. *Statistical Methods in the Atmospheric Sciences*, 3rd ed. International Geophysics Series, Vol. 100, Academic Press, 23–70.

Xia, Y., and Coauthors, 2012: Continental-scale water and energy flux analysis and validation for the North American Land Data Assimilation System project phase 2 (NLDAS-2): 1. Intercomparison and application of model products. *J. Geophys. Res.*, **117**, D03109, doi:10.1029/2011JD016048.

——, M. B. Ek, C. D. Peters-Lidard, D. Mocko, M. Svoboda, J. Sheffield, and E. F. Wood, 2014: Application of USDM statistics in NLDAS-2: Optimal blended NLDAS drought index over the continental United States. *J. Geophys. Res. Atmos.*, **119**, 2947–2965, doi:10.1002/2013JD020994.